Antiproton Slowing Down in H_2 and He and Evidence of Nuclear Stopping Power

M. Agnello,[1] G. Belli,[2] G. Bendiscioli,[3] A. Bertin,[4] E. Botta,[5] T. Bressani,[5] M Bruschi,[4] M. P. Bussa,[5] L. Busso,[5] D. Calvo,[5] B. Cereda,[4] P. G. Cerello,[5] C. Cicalò,[6] M. Corradini,[2] S. Costa,[5] S. De Castro,[4] A. Donzella,[2] A. Feliciello,[5] L. Ferrero,[5] A. Filippi,[5] V. Filippini,[3] A. Fontana,[3] D. Galli,[4] R. Garfagnini,[5] B. Giacobbe,[4] P. Gianotti,[7] A. Grasso,[5] C. Guaraldo,[7] F. Iazzi,[1] A. Lanaro,[7] E. Lodi Rizzini,[2] V. Lucherini,[7] S. Marcello,[5] U. Marconi,[4] A. Masoni,[6] B. Minetti,[1] P. Montagna,[3] M. Morando,[8] F. Nichitiu,[7,9] D. Panzieri,[5] G. Pauli,[10] M. Piccinini,[4] G. Puddu,[6] E. Rossetto,[5] A. Rotondi,[3] A. M. Rozhdestvensky,[9] A. Saino,[3] P. Salvini,[3] L. Santi,[11] M. G. Sapozhnikov,[9] N. Semprini Cesari,[4] S. Serci,[6] R. Spighi,[4] P. Temnikov,[6,9] S. Tessaro,[10] F. Tosello,[5] V. Tretyak,[3,9] G. L. Usai,[6] S. Vecchi,[4] L. Venturelli,[2] M. Villa,[4] A. Vitale,[1] A. Zenoni,[12] and A. Zoccoli[4]

[1]*Politecnico di Torino and Istituto Nazionale di Fisica Nucleare Sezione di Torino, I-10125 Torino, Italy*

[2]*Dipartimento di Chimica e Fisica per i Materiali, Università di Brescia, and Istituto Nazionale di Fisica Nucleare Sezione di Torino, I-25133 Brescia, Italy*

[3]*Dipartimento di Fisica Nucleare e Teorica, Università di Pavia, and Istituto Nazionale di Fisica Nucleare Sezione di Pavia, I-27100 Pavia, Italy*

[4]*Dipartimento di Fisica, Università di Bologna, and Istituto Nazionale di Fisica Nucleare Sezione di Bologna, I-40100 Bologna, Italy*

[5]*Istituto di Fisica, Università di Torino, and Istituto Nazionale di Fisica Nucleare Sezione di Torino, I-10125 Torino, Italy*

[6]*Dipartimento di Scienze Fisiche, Università di Cagliari, and Istituto Nazionale di Fisica Nucleare Sezione di Cagliari, I-09100 Cagliari, Italy*

[7]*Laboratori di Frascati dell'Istituto Nazionale di Fisica Nucleare, I-00044 Frascati, Italy*

[8]*Dipartimento di Fisica, Università di Padova, and Istituto Nazionale di Fisica Nucleare Sezione di Padova, I-35100 Padova, Italy*

[9]*Joint Institute for Nuclear Research, Dubna, SU-10100 Moscow, Russia*

[10]*Istituto di Fisica, Università di Trieste, and Istituto Nazionale di Fisica Nucleare Sezione di Trieste, I-34127 Trieste, Italy*

[11]*Dipartimento di Fisica, Università di Udine, and Istituto Nazionale di Fisica Nucleare Sezione di Trieste, I-33100 Udine, Italy*

[12]*Dipartimento di Chimica e Fisica per i Materiali, Università di Brescia, and Istituto Nazionale di Fisica Nucleare Sezione di Pavia, I-25133 Brescia, Italy*

(Received 15 June 1994)

We report stopping powers of hydrogen and helium for antiprotons of kinetic energies ranging from about 0.5 keV to 1.1 MeV. The Barkas effect, i.e., a difference in the stopping power for antiprotons and protons of the same energy in the same material, shows up clearly in either of the gases. Moreover, below ≈0.5 keV there is indirect evidence for an increase of the antiproton stopping power. This "nuclear" effect, i.e., energy losses in quasimolecular interactions, shows up in fair agreement with theoretical predictions.

PACS numbers: 34.50.Bw

At low projectile velocities ($\beta < 5 \times 10^{-2}$) significant differences in collision dynamics were observed [1,2] from one projectile-target system to another. In particular, the p and $\overline{p}$ stopping powers are expected to be very different around and below the stopping-power maximum where ionization and excitation decrease rapidly and the electronic capture channel for the proton becomes dominant [3]. In the velocity range $10^{-4} \leq \beta \leq 5 \times 10^{-3}$, quasimolecular effects come into play even more strongly and a $\overline{p}$ will lose energy both through nuclear collisions and through nonadiabatic ionization or excitation of the atom [3–9]. The $\overline{p}$ is predicted [5] to have the highest energy loss (the lowest being for μ^-) by such collisions between negative-charge projectiles and the atoms of the stopping medium. Moreover, a striking departure from velocity proportionality was reported for protons in He by Golser and Semrad [10] and well reproduced by Kimura [11].

In a previous work [2] we found that the stopping power of hydrogen is much smaller for $\overline{p}$ than for p (Barkas effect [12]) in the energy range from 10 to 120 keV. Moreover, a fast rise of the stopping-power behavior below 1 keV was needed to fit the data in the hypothesis that the capture energy of $\overline{p}$ lies in the electronvolt range.

We report here on the results of new measurements of the $\overline{p}$ stopping power both in hydrogen and helium. The measurements were performed by the OBELIX spectrometer at the CERN LEAR facility. In hydrogen, new data were taken at the pressures of 2, 5, 10, and 150 mbar [13]. In helium, the measurements were run at target pressures of 4, 8.2, 50, and 150 mbar.

By means of suitable thicknesses of material, the highly monocromatic $\overline{p}$ beam (with an energy of 5.875 MeV and an uncertainty of 10^{-3}) is degraded in order to obtain, at the entrance of the target, a beam with energy *continuously* distributed starting from $E_{\min} = 0$. Antiprotons enter the target ($z = 0$) at the time $t = 0$ and slowdown in a 0.5 T magnetic field oriented along the beam direction

(z axis), partly annihilating at rest in the gas and partly on the end wall of the target.

The mean annihilation-time values $\langle t_a \rangle$ versus corrected path lengths at different pressures in helium and hydrogen are shown in Fig. 1. Each point represents the position and the mean time at which annihilation takes place *at rest* in gas after the antiprotonic atom formation and the cascade on the nucleus. The z coordinate of the annihilation point is a measurement of the "projected" path length. In spite of this, the whole experimental information and Monte Carlo simulations make it possible to deduce that the mean "effective" path length is only slightly longer (our correction is $\langle 5\% \rangle$). Furthermore, in every z bin (1 or 2 cm wide) we observe no systematic difference between the $\overline{p}$ annihilation-time distributions for two different radial regions (i.e., $0 < r < 1.5$ cm and $1.5 < r < 4$ cm). The experimental accuracy is 1 cm and 1 ns, respectively, for the space and time coordinates in the target (30 cm in diameter and 75 cm long; entrance window radius 1 cm). We observe Gaussian annihilation time distributions along the target with the σ practically identical at any position, differing with the pressure.

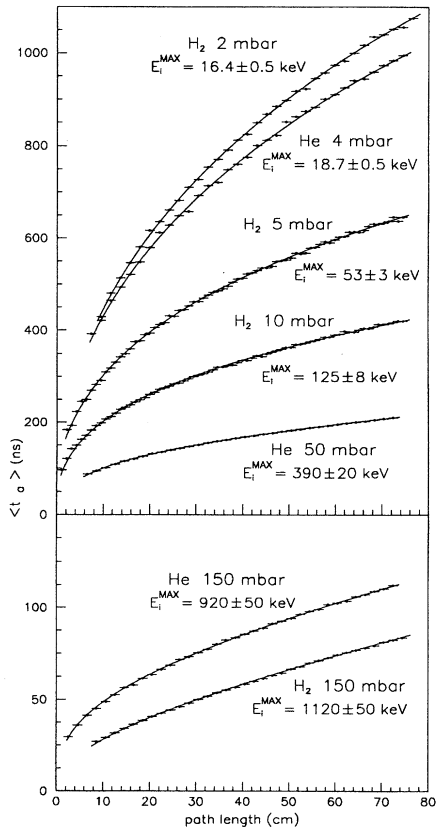

FIG. 1. Mean $\overline{p}$ annihilation time $\langle t_a \rangle$ versus corrected path length with the best fitting curves for different pressures in H_2 and He gases; the corresponding E_i^{MAX} values are also displayed.

Our technique makes it possible to evaluate the best-fit curves to the data, see Fig. 1, by using simultaneously the two following relations between the stopping-power function $S(E)$ and (i) the mean range $R(E)$,

$$R(E_i) = \int_{E_{cap}}^{E_i} \frac{dE}{S(E)}, \tag{1}$$

(ii) the mean moderation time $t(E_i)$,

$$t(E_i) = \int_{E_{cap}}^{E_i} \frac{dE}{vS(E)} = \langle t_a \rangle - \langle t_{cas} \rangle, \tag{2}$$

E_i being the $\overline{p}$ initial kinetic energy, v the instantaneous velocity, E_{cap} the $\overline{p}$ capture energy by the target atom, and $\langle t_{cas} \rangle$ the mean cascade time, of course constant at any annihilation point in the target gas and a free parameter in the fit to be matched with the experimental ones. The upper and lower experimental values for $\langle t_{cas} \rangle$ were evaluated at different pressures in both He and H_2. The upper limit was identified by means of the annihilation times in the target gas in the region close to the entrance window; the lower limit was inferred by the analysis of the different annihilation times in gas and aluminum at the end of the target (recall that the cascade times in solids are negligible with respect to those in our gases). The experimental limits for $\langle t_{cas} \rangle$ obtained in H_2 at 2, 5, and 10 mbar pressures are presented in Table I. E_i^{MAX} (E_i of $\overline{p}$ stopping at the end of the target) obviously decreases by lowering the target pressure and this represents an effective way to increase the sensitivity in $S(E)$ evaluated from (1) and (2) at even lower E values.

Hydrogen, energy range >0.5 keV.—In current low-energy theories, the electronic stopping power is found to be proportional to projectile velocity, i.e., $S_l = \alpha E^{\beta}$ with $\beta = 0.5$, while the high-energy behavior (S_h) is very well described by the Bethe formula. To bridge the gap between the high- and low-energy ranges, Varelas and Biersack [14] proposed a parametrization function S, given by $1/S = 1/S_l + 1/S_h$. For the case of hydrogen at 2 and 5 mbar pressures we obtain the best fit to the data by the function αE^{β} ("S_l") with $\alpha = 1.25$ and $\beta = 0.30$ down to $\approx$0.5 keV (see Fig. 1), where E is given in keV, E_i^{MAX} being about 53 keV at 5 mbar. For 10 and 150 mbar pressures good fits are obtained with the parametrization function S, where

$$S_h = (242.6/E)\ln(1 + \gamma/E + 0.1159E).$$

γ turns out to be 4×10^5, and E_i^{MAX} rises up to $\approx$1.1 MeV at 150 mbar pressure.

In Fig. 2(a) the $\overline{p}$ stopping-power best fitting function $S(E)$ ($\chi^2 = 0.37$) obtained for H_2 is reported, compared

TABLE I. Lower and upper limits for the cascade times of $\overline{p}p$ atoms formed at different hydrogen densities.

H_2 press (mbar)	2	5	10
$\langle t_{cas} \rangle$ (ns)	140 to 190	90 to 130	45 to 65

to the proton and the μ^- ones, the band of the maximum error being around 10% down to 0.5 keV.

At any pressure the upper- and lower-limit stopping powers down to ≈0.5 keV [dashed lines in Fig. 2(a), $\chi^2 \approx 3$ to 4 times higher than the best one] clearly disagree with the actual one *crossing* the experimental values, see Figs. 1 and 3. For the lower limit in S_l we obtain $\alpha = 1.15$, $\beta = 0.30$, and $\gamma = 10^5$, and for the higher limit $\alpha = 1.30$, $\beta = 0.31$, and $\gamma = 8 \times 10^5$.

Regarding the behavior above the maximum of the electronic stopping power our best fit indicates a higher stopping power for $\overline{p}$ than for p, the difference being at the limit of the present experimental uncertainty.

Hydrogen, energy range <0.5 *keV.*—To evaluate $S(E)$ in the very low-energy region ($E \leq 0.5$ keV) we observe, from Eq. (2), that globally low $S(E)$ values would imply high moderation times at $t(E_i)$ and consequently low $\langle t_{\rm cas}\rangle$ value at that pressure, the sum having to be $\langle t_a\rangle$. Therefore, it is not surprising that a behavior for $S(E)$ assumed from the extrapolated value of our αE^β function down to the capture energy (≈5 eV) would result for the 2 mbar H_2 pressure in a *negative* mean cascade time, while it would turn out to be around 40 ns for a constant $S(E)$ value below ≈0.5 keV [dot-dashed lines in Fig. 2(a)]. Also the cascade times related to the dashed limiting stopping-power behaviors below ≈0.5 keV disagree with the experimental ones (see Table I) for the three pressures considered (compare the values reported in Fig. 3 to the experimental ones).

In Fig. 2(b), the dashed line below the minimum is coherent with the behavior predicted by Wightman [5], while the dot-dashed one is inspired by the Morgan behavior [6]. The first one gives good fits to the data and $t_{\rm cas}$ results in ≈120 ns at 2 mbar pressure, which is a bit low. It rises to ≈155 ns with the dot-dashed Morgan-like curve, the fits being, however, fairly worse. Good fits to the data and $t_{\rm cas} \approx 150$ ns are obtained also with the dotted curve in Fig. 2(b), which is a pure analytical function without specific physical meaning.

Helium.—For the case of helium the procedure is just the same. At the lowest pressures (4 and 8.2 mbar) our fitting function looks like αE^β with $\alpha = 1.45$ and $\beta = 0.29$ down to ≈0.5 keV (S_l). For 50 and 150 mbar pressures we use the same parametrization function S as

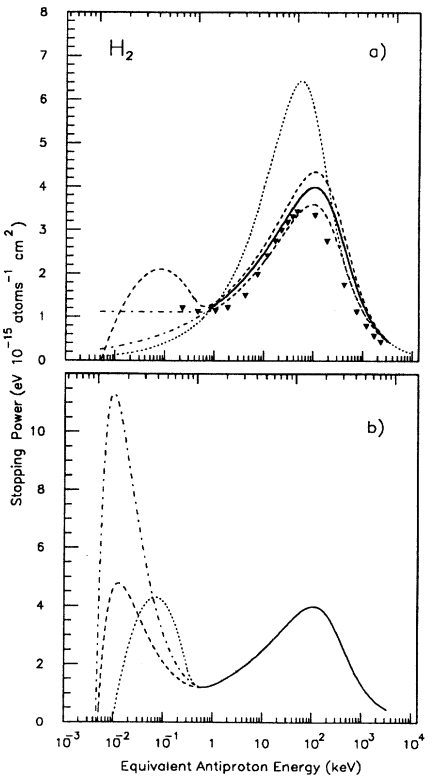

FIG. 2. (a) $\overline{p}$ stopping-power best fitting function in H_2 (solid line), with the upper- and lower-limiting behaviors down to 0.5 keV (dashed lines); proton behavior [10] (dotted line); ▼: μ^- data [14]. Below 0.5 keV three unacceptable behaviors are presented. (b) $\overline{p}$ stopping-power best fitting function in H_2 (solid line) down to 0.5 keV with three acceptable behaviors below 0.5 keV.

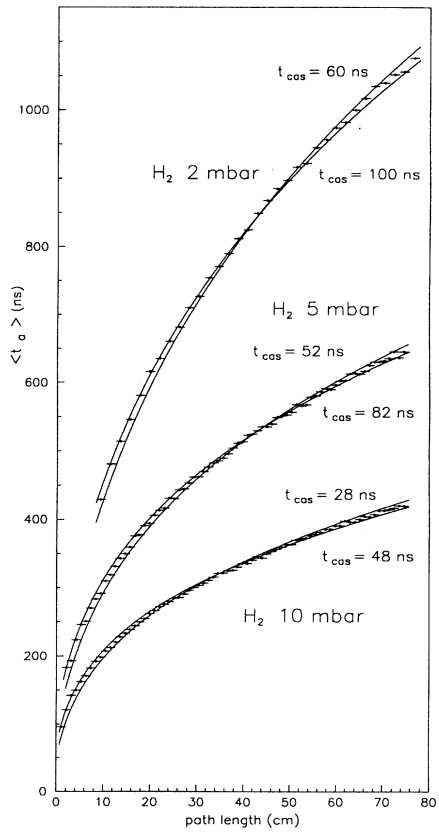

FIG. 3. Mean annihilation time $\langle t_a\rangle$ versus corrected path length with the two limiting behaviors [yielding the dashed lines in Fig. 2(a)], for H_2 at three pressure values.

for H_2 where

$$S_h = (484.5/E)\ln(1 + \gamma/E + 0.05225E)$$

up to $\approx$1 meV and γ results in 2×10^5. The ratio between γ(He) and $\gamma(H_2)$ is similar to that for the proton ($\approx$0.5) [15]. Moreover, the γ values are a factor $\approx$35 higher in the $\overline{p}$ case.

A rise below the minimum $\approx$0.5 keV is needed too, and in Fig. 4 we report possible $\overline{p}$ stopping-power behaviors with an attitude similar to the one assumed for Figs. 2.

In conclusion, important issues can be answered by the present results for (i) particle-antiparticle behavior of the stopping powers in light targets and (ii) $\overline{p}$-μ^- comparison.

As far as point (i) is concerned, the following is evidenced out by the present work:

(a) *The stopping-power behaviors for $\overline{p}$ in H_2 and He are similar* also below the maximum, and quite different from the proton's ones as measured by Golser and Semrad [10].

(b) *Within the energy range from 1–2 up to about 250 keV,* the $\overline{p}$ stopping power is smaller than the p one (see Ref. [16] for higher-Z elements like Si and Au). The differences are significant, the stopping power being $\approx$62% and $\approx$67% of the proton one at the maxima in hydrogen and helium, respectively. The maxima for the $\overline{p}$'s are also shifted toward higher energies ($\approx$100 keV in H_2 and $\approx$120 keV in He).

(c) *Below $\approx$0.5 keV,* an increase of the $\overline{p}$ stopping power is necessary in order to agree with the present experimental results, although their resolution does not yet allow a choice in favor of a well defined stopping-power behavior. In any case, the $\overline{p}$ "nuclear" stopping power is in qualitative agreement with the predictions by Wightman [5] and Morgan [6].

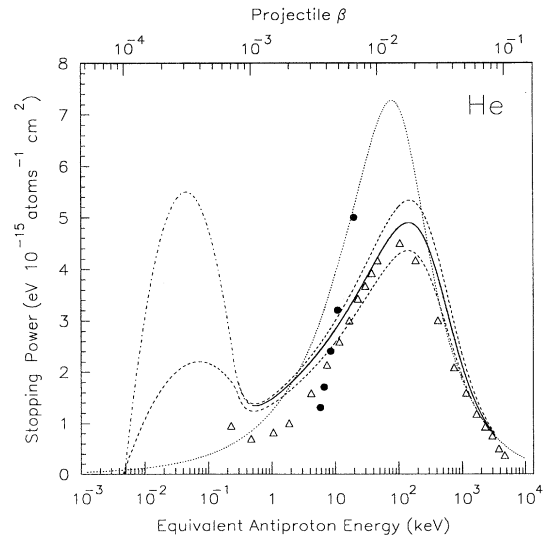

FIG. 4. $\overline{p}$ stopping-power best fitting function for He (solid line) and upper- and lower-limiting behaviors down to 0.5 keV (dashed lines); the dotted line is the proton stopping power [10]; ●: Golser and Semrad data [11]; △: μ^- in He [13]; dot dashed and dashed lines below 0.5 keV are, respectively, an acceptable and an unacceptable behavior for $\overline{p}$ stopping power.

As to point (ii), the comparison between $\overline{p}$ and μ^- [17,18], see Figs. 2(a) and 4, shows that their behaviors are qualitatively very similar down to 1 keV. On the left of the minima the μ^- stopping powers are unknown, but we recall here the predictions by Wightman (see, e.g., Fig. 2 in Ref. [4]), who suggested a very different nuclear stopping power contribution in the region $\beta < 5 \times 10^{-3}$ for $\overline{p}$, k^-, π^-, and μ^-, the one for muons being very small.

Very good agreements with the present data were recently obtained by the Cyclotron Trap Group working at LEAR [19] by comparing the experimental moderation times both in He and in H_2 for $\overline{p}$'s around 1 MeV initial kinetic energy stopping in gases at different pressures ranging from 2.5 to 20 mbar with those evaluated by using our stopping power behaviors.

We are indebted to Professor J. Lindhard and Professor A. H. Sorensen for useful suggestions and critical remarks.

[1] H. Knudsen and J. F. Reading, Phys. Rep. **212**, 107 (1992).
[2] A. Adamo *et al.,* Phys. Rev. A **47**, 4517 (1993).
[3] G. Schiwietz, Phys. Rev. A **42**, 296 (1990).
[4] N. Bohr, Mat. Fys. Medd. Dan. Vidensk. Selsk. **18** (1948).
[5] A. S. Wightman, Phys. Rev. **77**, 521 (1950).
[6] D. L. Morgan, Jr., Hyperfine Interact. **44**, 399 (1988).
[7] A. M. Ermolaev, Hyperfine Interact. **44**, 375 (1988).
[8] M. Kimura and M. Inokuti, Phys. Rev. A **38**, 3801 (1988).
[9] P. Hvelplund *et al.,* J. Phys. B **27**, 925 (1994).
[10] R. Golser and D. Semrad, Phys. Rev. Lett. **66**, 831 (1991).
[11] M. Kimura, Phys. Rev. A **47**, 2393 (1993).
[12] W. H. Barkas, J. N. Dyer, and H. H. Heckman, Phys. Rev. Lett. **11**, 26 (1963).
[13] The measurements at 2, 5, and 10 mbar were repeated, since the previous ones [2] were reported with an error in the pressure scale (about 1.5 mbar lower than the actual one).
[14] C. Varelas and J. P. Biersack, Nucl. Instrum. Methods **79**, 213 (1970).
[15] *Hydrogen Stopping Powers and Ranges in All Elements,* edited by H. H. Andersen and J. F. Ziegler (Pergamon, New York, 1977).
[16] R. Medenwaldt *et al.,* Phys. Lett. A **155**, 155 (1991).
[17] P. Hauser *et al., Muonic Atoms and Molecules* (Birkhauser, Verlag, Basel, 1993), p. 235.
[18] P. Baumann *et al.,* PSI Nuclear and Particle Physics Newsletter **59** (1992).
[19] D. Horvath *et al.,* in Proceedings of the VI Workshop on Atoms, Molecules and their Interactions, Erice, 1994, edited by G. Pauli, C. Rizzo, and E. Zavattini (to be published).